Modeling, Integration and Simulation of the Photovoltaic Power Plant Considering LVRT Capability and Transient Voltage Stability

ABDELAZIZ SALAH SAIDI[1,2] (Member, IEEE), OSAMA ALI ZEMI[3], LINA ALHMOUD[4], and MUHAMMAD UMAR MALIK[5]

[1] Electrical Engineering Department, King Khalid University, Abha 61421, KINGDOM OF SAUDI ARABIA

[2] Laboratoire des Systèmes Electriques, Ecole Nationale d'Ingénieurs de Tunis,
Université de Tunis El Manar, TUNISIA

[3] National Grid company, Project Management Office, Central Operation Area, KINGDOM OF SAUDI ARABIA

[4] Electrical Power Engineering Department, Hijjawi Faculty for Engineering Technology, Yarmouk University, Irbid 21163, JORDAN

[5] Grid Studies Department, National Grid Company, KINGDOM OF SAUDI ARABIA

Abstract: - This paper investigates how high photovoltaic energy penetration impacts dynamic performance and voltage regulation of the modified IEEE-9 bus grid. The transmission power system was modeled and simulated using PSCAD-EMTDC software to conduct the study. Load flow analysis is implemented to explore the power system's capability to incorporate the desired photovoltaic power. Moreover, the study is based on time response simulations to grid disturbances. The supply and control of reactive power from solar power generation plants are becoming critical issues to study because they can facilitate the integration of PV in power grids under different operating conditions. Network-related faults like a PV solar power plant event outage, a three-phase short-circuit at a conventional bus, and a voltage dip at the PV solar power plant have been considered. The results will help identify the protective devices and strategies needed to maintain the stability and reliability of the system operation and transient analysis of the network under external power network fault and recovery operation. Thus, it has practical significance for real utility studies. Moreover, this comprehensive study will be a valuable guide for assessing and improving the grid's performance under the study of any other grids, which also gives the vast potential and need for solar energy penetration into the grid systems.

Key-Words: - Photovoltaic power plant, PSCAD, Static load, Modeling, Transient voltage stability, LVRT capability.

Received: November 23, 2022. Revised: November 24, 2023. Accepted: December 27, 2023. Published: December 31, 2023.

1 Introduction

Voltage stability is the ability of the system to preserve acceptable voltages at all buses in the system under normal conditions, especially after being exposed to a disturbance. A power system is said to have gotten into a state of voltage instability when a disturbance results in a progressive and uncontrollable very low voltage. The power system may undergo voltage collapse if the post-disturbance equilibrium voltages near loads are below acceptable limits. Voltage collapse is a process that leads to a decline in voltage profile, causing voltage instability in a significant part of the system. Voltage stability is sometimes called load stability [1]. The present transmission systems are increasingly stressed due to economic and environmental constraints. Voltage stability problems usually occur in heavily stressed systems. Thus, voltage security means the ability of a system not only to operate stable but also to remain stable following a contingency or load increase. Voltage stability can be classified based on time frame: short-term voltage stability and long-term voltage stability; and the type of disturbance: small disturbance voltage stability and significant disturbance voltage stability [2]. Short-term voltage stability typically lasts for a few seconds. The analysis requires a solution of appropriate differential equations. It involves dynamics of fast-acting components such as automatic voltage regulator (AVR), turbine, and governor dynamics. Long-term voltage stability is mainly due to the considerable distance between the generator and the load. It involves the dynamics of slow-acting equipment such as a tap-changing transformer. The time frame is within a few minutes to tens of minutes. This type of voltage instability may be prevented by load shedding and reactive power compensation [3].

Large disturbance voltage stability measures the system's ability to control voltage at all buses following significant disturbances such as generation loss, load loss, and systems faults. This stability can be determined by assessing the system's dynamic performance over sufficient time to capture device interactions such as generator field current limiter and unload tap changing transformers. Meanwhile, in small-distance voltage stability, following any minor disturbances at any given operating state, the voltage close to the load remains fixed or near the pre-disturbance values [4]. The load flow study is the first step in analyzing the power system from the capacity standpoint to investigate generation sources, transformers, and cables that match the intended loads. In addi-

tion, a load flow study points out locations in the system where low-voltage or high-voltage conditions may exist. The first step in a load flow study is to create an accurate system model in a line diagram. Computer programs like PSCAD can run simulations on that power system to evaluate what-if scenarios for load changes in contingent situations [5]. The iterative process of a load flow simulation starts by using the load as a known quantity. Still, since current flow is likely based on voltage and the voltage at a particular node varies based on current flow, the program needs to make an educated guess as to the total power flowing from the source. Then, calculations are performed until the mismatch of the estimation is very close to the actual load specified. The load flow simulation solves losses and voltage profiles [5], and bold changes along the way are plotted on a single-line diagram. Scenarios are created to determine if new equipment is needed or if transformer tabs need to be adjusted to compensate for the additional load. The benefit of this study is that if the network size is increased or new renewable generation sources are added, starting from the base case model of the system, Many alternative scenarios can be run until the results are comfortable. At the end of this process, the operator knows precisely the required changes needed to optimize power flow and cost. Ways can be shown to reduce energy bills or how to add more load to the existing system for capacity reasons, voltage drop consideration, or loss calculations to enhance transient voltage stability profile while improving voltage levels throughout the system [6].

Power system stability and control are not considered new concerns. However, grid operators are now paying extra attention to keeping the transmission systems stable to prevent the recurrence of large blackouts that have affected many countries. Thus, the power system network is under typical operating conditions, and after being perturbed, it should be sustained, stable, reliable, and secure, and the bus voltages should be within limits. There are several ways to approach voltage stability study [6]. However, it can be helpful for operators to estimate the power system's closeness to voltage collapse before implementing corrective measures and taking premedical actions. Voltage stability analysis is still frequently used in industries to calculate the P-V and Q-V curves at specific load buses [7]. Numerous load flows often produce these curves utilizing traditional techniques and models. However, these techniques take a lot of time and don't offer enough valuable information to address the stability issues. In [8], several reasons electricity systems go through interruptions are listed. Meanwhile, power system outages can be prevented in several cases with sufficient system protection and adequate awareness. Suppose the power system is not equipped with suitable protection for the system [9]. In that case, the power system is prone to unexpected factors such as external disturbances, component failures, and parameter changes [9]. Hence, voltage instability is one of the problems causing power interruptions and voltage collapse. The power system utilized in this paper is the IEEE 9-bus test case. The IEEE 9-bus test case represents a portion of the Western System Coordinating Council (WSCC) [2], [10]. Many researchers have studied it and a PV solar power plant connected to bus 6. Integration of PV solar power plants poses significant challenges. Thus, it limits reactive power capability and causes a significant voltage drop or rise in the system [11], [12].

The work assesses transient voltage stability in a modified IEEE 9-bus in the presence of a photovoltaic (PV) solar power plant and a three-phase short circuit at the most loaded bus in the system. The system was modeled in PSCAD; a simulation study was performed to investigate potential transient voltage stability based on the voltage profiles, active and reactive power profiles, and system stability. The system under different operating conditions is simulated and analyzed. It aims to classify stability issues likely to occur in the grid by identifying different scenarios to enhance the industry's understanding of the interaction of PV solar power plants with other assets in the system. In this work, the IEEE 9-bus is used to create an equivalent standard test in PSCAD. The power flow data system is available in [2]. After successfully validating the power flow, many scenarios are simulated. (i) the pre-disturbance steady state is obtained, (ii) a PV solar power plant is integrated into the system at bus 8, and the dynamic performance is registered, (iii) the impact of a three-phase short circuit takes place at the most loaded bus 8 while a sudden disconnection of the PV solar power plant is simulated and discussed. (iv) The impact of a three-phase short circuit occurs at the most loaded bus 8 while reconnection of the PV solar power plant is analyzed.

The paper is organized such that Section 2 presents the implementation of a PV solar power plant in PSCAD. Section 3 describes the proposed system understudy of IEEE 9-bus before and after modifications. Section 4 presents the results of four scenarios: base case, modified case with PV solar power plant, modified case with PV solar power plant connected at bus 6, and three-phase short circuit at bus 8 which is the most loaded bus. Finally, the case after the sudden disconnecting of the PV solar power plant in the presence of a fault of a three-phase short circuit. Section 5 presents the conclusion and future work.

2 PV plant model and control

PSCAD (Power Systems Computer Aided Design) is a commercial international software for analyzing

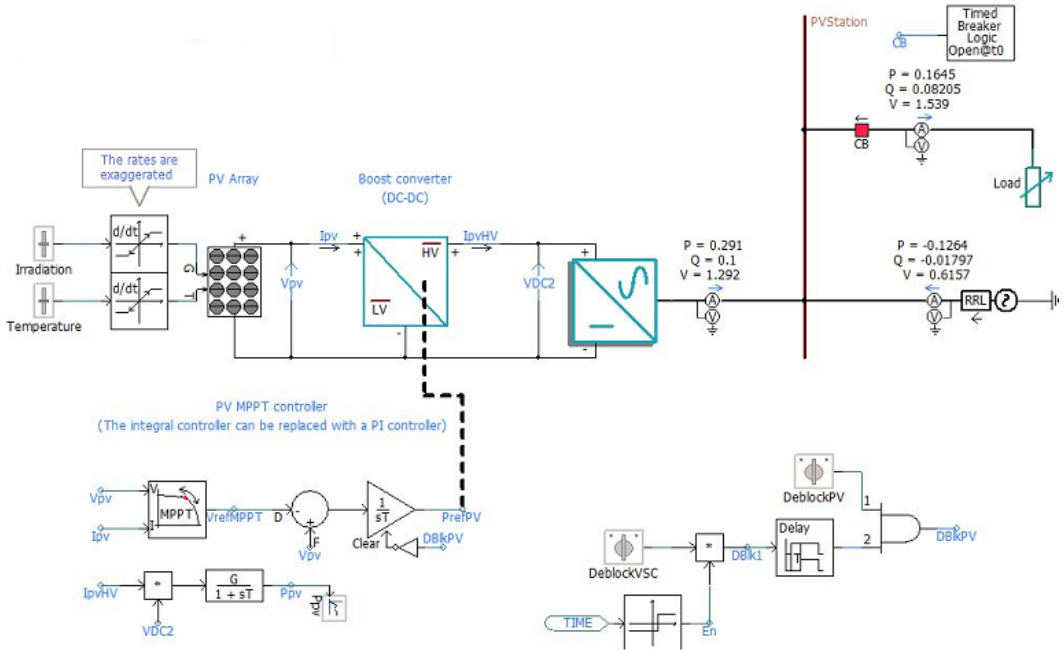

Figure 1: Grid-connected PV plant model using PSCAD software [13].

and simulating power and electrical systems. It was officially developed by the engineering department within Manitoba Hydro International Ltd. (MHI) in 1983 in Canada. It is a comprehensive building, modeling, and simulating electromagnetic transient (EMT) studies. It includes an extensive library of power and energy models, including passive elements, control functions, and electrical machines. The integrated calculations and analysis software, power flow calculation, short circuit calculation, motor starting, and transient stability. Models include power system studies, HVDC and FACTS, renewable energy integration, electromagnetic transient studies, and power equipment services. Thus, it introduces a comprehensive and robust solution from simulation to real-time operational control for power generation, transmission systems, distribution, and utilization. The functional expressions in each module are very intuitive and easy to understand. Each part's simulation modules' simulation results can also be given as a report [13], [14].

Integrating PV solar power plants in PSCAD is available under different operating conditions. There are two switches, one to control the irradiation and the other to control the temperature. The PV solar power plant model mainly consists of arrays and converters as shown in Figure 1. The PV Array is a PSCAD module used to model the behavior of a solar photovoltaic (PV) array. It typically contains a group of solar PV panels connected in series and parallel to generate the system's required DC voltage and current. The main function of the PV Array during the simulation of a PV solar power plant is to model the behavior of the solar PV array and its interaction with the other components in the system, such as the boost converter, voltage source converter, and LCL filter. Precisely, the PV Array Box in PSCAD can model the behavior of the solar PV array by generating DC power based on the input irradiance and temperature values. The DC power output is then sent to the boost converter for voltage regulation. In addition, it can monitor the DC voltage and current of the solar PV array to ensure that they remain within the system's operating range. The PV Array Box can model the behavior of the individual PV panels in the array by considering their temperature coefficient, shading effects, and other factors that affect their performance. The PV Array Box can implement MPPT algorithms to optimize the power output of the solar PV array by adjusting the input voltage and current to ensure that the PV panels operate at their maximum power point [15], [16].

The specific settings and parameters of the voltage source converter (VSC) in PSCAD may vary depending on the characteristics of the solar PV system and the power grid. Therefore, it is essential to carefully analyze the behavior of the solar PV system and adjust the VSC settings accordingly to ensure proper performance during the simulation. The boost converter is a DC-DC converter commonly used in solar PV systems to step up the DC voltage produced by the PV panels to a suitable level for the voltage source converter (VSC) [17]. The main function of the boost

converter during the simulation of a PV solar power plant is to regulate the DC voltage to ensure that it remains within the range required by the VSC. The boost converter does this by adjusting the switch's duty cycle to control the current flow through an inductor and a capacitor. The boost converter can also provide other essential functions, such as maximum power point tracking (MPPT), to optimize the power output of the PV solar power plant by adjusting the input voltage and current to ensure that the PV panels operate at their maximum power point. Besides, the boost converter can limit the input current to the VSC or inverter to ensure that it remains within the rated capacity of the device and does not cause overloading or damage [18]. Also, the boost converter can detect and protect against faults, such as overvoltage, undervoltage, overcurrent, and short-circuit conditions, to ensure that the PV solar power plant operates safely and reliably. Besides, the VSC can adjust the phase angle between the current and voltage waveforms to improve the system's power factor, reducing losses and improving the system's efficiency. Also, the VSC can detect when the power grid is disconnected or experiences a fault and automatically switch to islanding mode to ensure that the PV solar power plant continues supplying power to critical loads. The VSC can suppress the high-frequency harmonics generated to ensure that the AC power injected into the grid meets the relevant power quality standards [19].

3 System Under Study

The IEEE 9-bus system is a standard test case used in power system analysis and research [1]. It consists of nine buses, three generators, three loads, and transmission lines and transformers, as shown in Figure 2. Table 1,Table 2, and Table 3 summarize the per unitized terminal conditions of each source, the transmission lines parameters, and PQ load model with 100 MVA, respectively. The base voltage levels are 16.5 kV, 13.8 kV, 18 kV, and 230 kV. The complex power for each line is around hundreds of MVA each. The generators are connected to Bus 1, Bus 2, and Bus 3. Meanwhile, the loads at Bus 5, Bus 6, and Bus 8. This system has a few voltage control devices. Thus, it is easy to control. The purpose of the IEEE 9-bus system is to provide a standard reference for researchers to test and compare new power system analysis techniques, such as load flow, transient stability, and fault analysis. The system is also used for teaching purposes in power system courses. Researchers use IEEE 9 bus systems to implement new ideas and concepts. Indeed, the test was developed by the Western System Coordinating Council (WSCC). In transient stability studies, it is vital to have the pre-fault voltage magnitude and phase angle at each bus and active and reactive power on generation and transmission buses.

Table 1: Conditions of the IEEE 9-bus system.

Bus	V (kV)	δ^o	Active power (pu)	Reactive power (pu)
1	17.160	0.0	0.7163	0.2791
2	18.45	9.3507	1.63	0.049
3	14.145	5.142	0.85	-0.1145

Table 2: Transmission line characteristics of IEEE 9-bus system.

From line	To line	R (pu/m)	X (pu/m)	B (pu/m)
4	5	0.0100	0.0680	0.1760
4	6	0.0170	0.0920	0.1580
5	7	0.0320	0.1610	0.3060
6	9	0.0390	0.1738	0.3580
7	8	0.0085	0.0576	0.1490
8	9	0.0119	0.1008	0.2090

Table 3: Load characteristics of IEEE 9-bus system.

Bus	Active power (pu)	Reactive power (pu)
5	1.25	0.50
6	0.90	0.30
8	1.00	0.35

A 25 MW PV system testbed is adopted to observe the LVRT dynamics. This model was developed and posted by PSCAD [13]. The system topology is shown in Figure 2. The solar farm consists of 100 PV arrays. Each unit generates a maximum power of 0.25 MW at the nominal irradiation of $1000W/m^2$ and nominal temperature of 28^o. The MPPT, detailed DC/DC boost converter, and detailed three-phase switches are included, shown in Figure 1. The system parameters are given in Table 4. The base voltage on the DC side is 1 kV. The DC voltage is converted to 0.55 kV AC voltage through GSC.

4 Simulation results and discussions

4.1 Steady state voltage stability

In load flow analysis, PV solar power plants are usually integrated into the generator-type PV bus because of their voltage control capability and due to the active power generation [20]. On the other hand, they are considered load buses after achieving their reactive generation limits. Each PV solar power plant has been characterized in the power system based on the above hypothesis. The PV solar power plant is synchronized with a grid by having inverters. They do not provide voltage and frequency as a reference by themselves when connected to the electrical installation. They measure the voltage and frequency

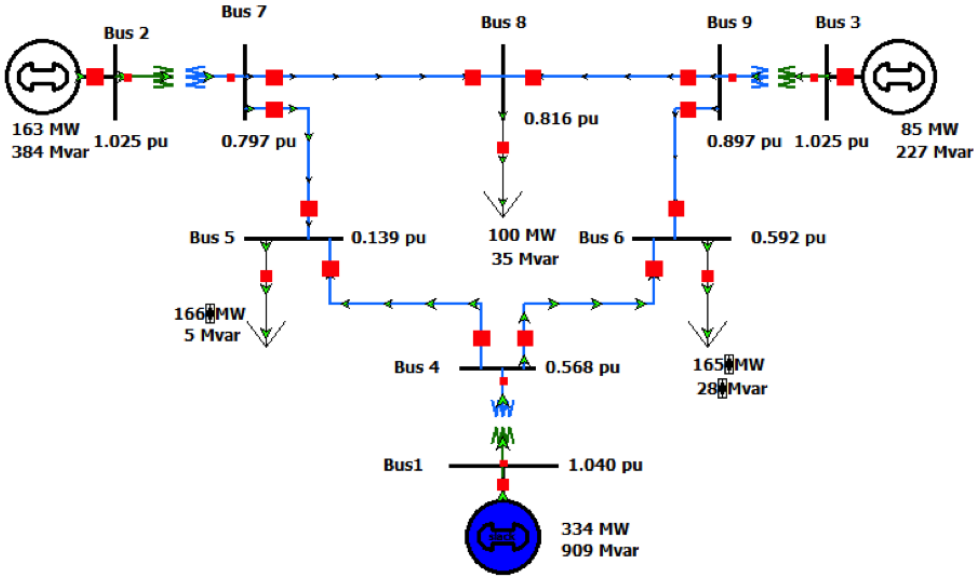

Figure 2: IEEE 9- bus test systems [10].

Table 4: 25 MW PV solar power plant PSCAD testbed parameters.

Description	Parameters	Value
Switching frequency	3 kHz (VSC)	5 kHz (DC-DC)
Power base	S_b	25 MW
Inverter power base	S_b'	250 kW
Inverter dc voltage base	$V_{DC,b}$	1 kV
PCC voltage base	$V_{PCC,b}$	0.55 kV
POC voltage base	$V_{POC,b}$	33 kV
Power level	$P_{POC,b}$	1 pu
System frequency	f_b	60 Hz
LCL filter	L_{filter}, C_{filter}	0.32 mH, 54.80 μF
Damper	L_{damp}, C_{damp}, R_{damp}	1.60 mH, 27.40 μF, 7.65 Ω
Shunt capacitor	B_{C1}	0.2 pu
DC-link capacitor	C_{dc}	10000μF
PV LC filter	L_{PV}, C_{PV}	2.5 mH, 100μF
Transformer impedance	X_{T1}	0.05 pu
Transmission line	X_g, R_g	0.45 pu, 0.05 pu
Current control loop	K_{pi}, K_{ii}	(0.2, 20) pu
DC-link control loop	K_{pp}, K_{ip}	(1,20) pu
V_{AC} Control loop	K_{pv}, K_{iv}	(1,10) pu
PLL	$K_{p,PLL}$, $K_{i,PLL}$	(500,200) pu

at their connection point and deliver a power output synchronized with this voltage and frequency of the grid. Here, the inverters should be designed to have no mismatches or instability in the electrical installation. In this work, the system voltage profile for peak load conditions has been tested with and without connection to a PV solar power plant. The characteristic of the voltage profile at all IEEE 9-bus systems with and without PV solar power plants are shown in Table 5 and Figure 3. The bus voltage ranged from 0.995 to 1.028 pu at zero PV solar power plant connection case. The voltage magnitude profile was improved by integrating the PV solar power plant and injecting the maximum power point tracking. It was observed that the voltage magnitude was increased, but no overvoltage was observed after integration for all busbars. Remarkably, the grid voltage profile increased from 1.005 pu to 1.045 pu. In most of the buses in the system, the voltage profile is within the 5% tolerance. The terminal voltage phase angle at each connection bus is measured in degrees for the system without and with a PV solar power plant and presented in Table 5. It can be perceived that the voltage angles of neighboring buses are nearly identical, as demonstrated by numerous references [6].

The base case results of load flow analysis of static stability are given in Table 5 and Table 6, respectively. The results show that MVAR losses are higher than the MW losses. This is because the reactance values are greater than the resistive values, as shown in Table 2. In the transmission lines, the active power can transfer between the sending end and the receiving end in the transmission lines. The overloads on highly loaded feeders and capacity release on these feeders and substations are alleviated through the significant penetration of PV solar power plants. There is a minimization of total distribution power losses. When connecting solar PV solar power plants, the power losses moderately decrease compared with the normal system power losses; thus, power losses versus the penetration rate of the solar PV system.

Figure 4, Figure 5, Figure 6, Figure 7, Figure 8, Figure 9, Figure 10, Figure 11, Figure 12, and Figure 13 show the steady state analysis (base case) for

Table 5: The busbar voltage (pu) for the IEEE 9-bus system with & without PV power plant connected.

Bus	Bus voltage(pu)	Bus angle (^{o})	Bus voltage (pu)	Bus angle (^{o})
Bus 1 (swing)	1.036	4.1	1.045	5.1
Bus PV	-	-	1.032	-
Bus 2	1.02	8.5	1.032	11.0
Bus 3	1.02	4.9	1.029	6.3
Bus 4	1.021	-3.3	1.005	0.12
Bus 5	0.995	-5.0	1.012	-2.0
Bus 6	1.007	4.98	1.035	-0.12
Bus 7	1.022	-1.0	1.024	2.5
Bus 8	1.012	0.9	1.038	3.2
Bus 9	1.028	2.2	1.045	4.97

Table 6: The base case of load flow analysis for IEEE 9-bus system via. losses in transmission lines with & without PV solar power plant connected.

From Bus	To Bus	Without PV		With PV	
		Losses (MW)	*Losses (MVAR)*	*Losses (MW)*	*Losses (MVAR)*
Bus 4	Bus 5	0.33	-15.94	0.3	-16.23
Bus 4	Bus 6	0.16	-15.458	0.09	-16.064
Bus 5	Bus 7	-2.19	0.643	1.98	5.382
Bus 7	Bus 8	0.51	-11.06	0.46	-12.6851
Bus 8	Bus 9	-0.08	21.148	-0.10	21.5601
Bus 9	Bus 6	1.52	4.4	1.14	-6.41

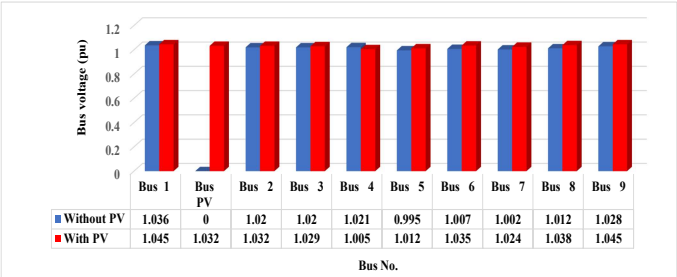

Figure 3: Bus bar voltage for the system under study with & without PV solar power plant.

the system under study. Figure 4 shows the active power generation at bus, Figure 5 shows the active power generation at bus 2 & bus 3. Figure 6 shows the reactive power generation at bus 1, Figure 7 shows the reactive power generation at bus 2 & bus 3, Figure 8 shows the bus voltage at all buses, Figure 9 shows the active power at load bus 5 & bus 8, Figure 10 shows the active power at load bus 6, Figure 11 shows the reactive power at load buses 5 & bus 8, Figure 12 shows the reactive power at load bus 6, Figure 13 shows the bus angle at all buses. The dynamic voltage stability of the studied power system was examined by assessing the behavior of the voltage at the buses during the normal conditions. The simulation results show that the solutions of the dynamic power system model converge to the equilibrium characterized by the nominal voltage as well as active and reactive power generation and consumed. The results indicate also that the system is stable with respect to the same voltage, reactive and active power solved by the load flow analysis in the previous section.

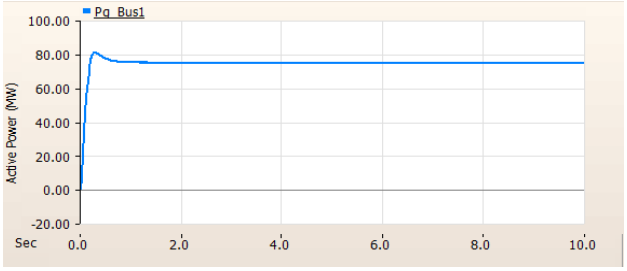

Figure 4: Active power generation at bus 1- base case (MW).

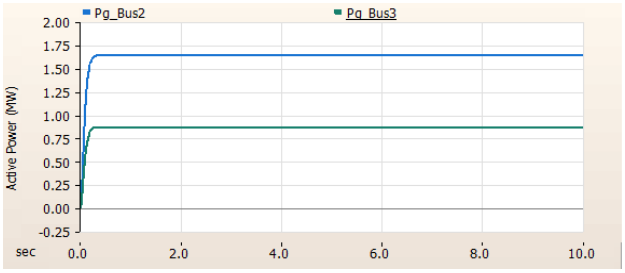

Figure 5: Active power generation at bus 2 & bus 3- base case (MW).

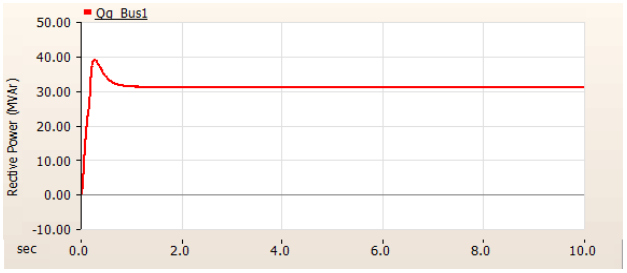

Figure 6: Reactive power generation at bus 1- base case (MVAR).

4.2 Dynamic performance

4.2.1 PV power plant disconnection

A base case scenario of PV solar power plants connected to bus 6 in the IEEE 9-bus system is analyzed as shown in Figure 14. Here, the initial conditions

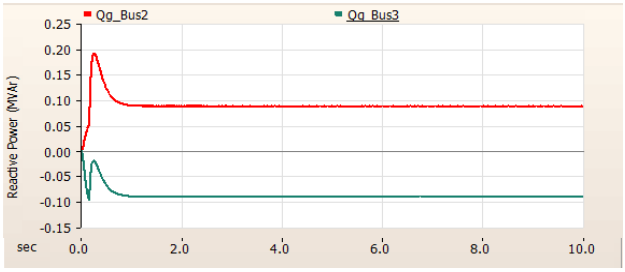

Figure 7: Reactive power generation at bus 2 & bus 3- base case (MVAR).

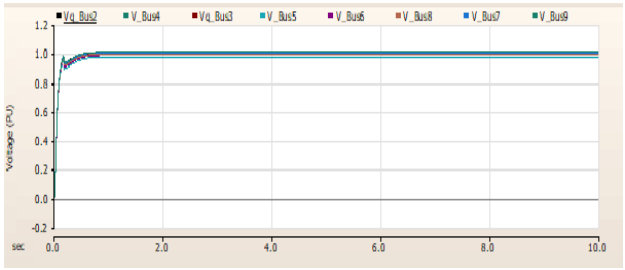

Figure 8: Bus voltage (pu) at all buses- base case (MW).

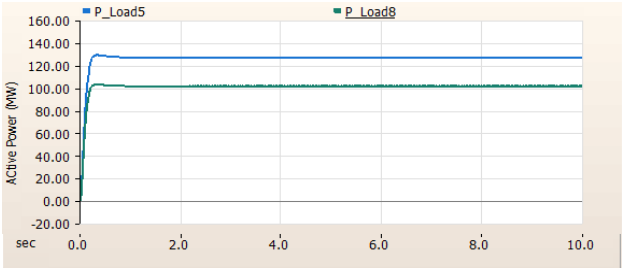

Figure 9: Active power at load bus 5 & bus 8 base case (MW).

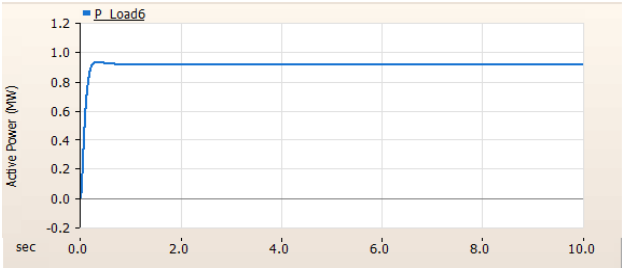

Figure 10: Active power at load bus 6- base case (MW).

have been set for 100% power output of the PV nominal power at standard test condition (STC) at $25°C$ cell temperature, $1000W/m^2$ solar radiation, and air mass of 1.5. Figure 15, Figure 16, Figure 17, Figure 18, Figure 19, Figure 20, Figure 21, Figure 22, Figure 23, and Figure 24 show the dynamic perfor-

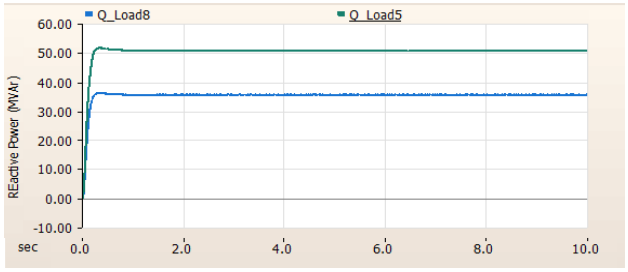

Figure 11: Reactive power at load buses 5 & bus 8- base case (MVAR).

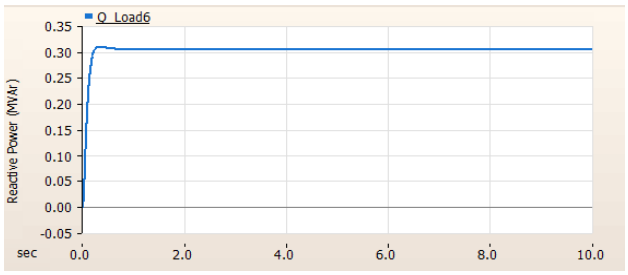

Figure 12: Reactive power at load bus 6- base case (MW).

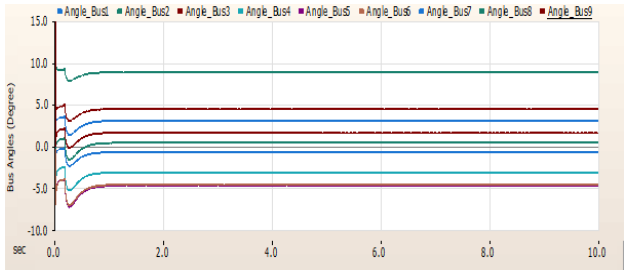

Figure 13: Bus angle at all buses-base case.

mance analysis for the system under study with the PV solar power plant connected to bus 6. During this base case scenario, the voltage response at all buses converges to the equilibrium nominal per-unit values with and without a PV solar power plant connection. Figure 15 and Figure 16 show the reactive power generation at the synchronous generator power plant swing bus 1 and the solar PV generator bus 2 equals 60 MW and 30 MW, respectively. Figure 17 and Figure 18 show the reactive power generation at the synchronous generator power plant swing bus 1 and the solar PV generator bus 2, respectively. Figure 19 shows the bus voltage at all buses, Figure 20 shows the active power at load bus 5 & bus 8, Figure 21 shows the active power at load bus 6, Figure 22 shows the reactive power at light load buses 5 & bus 8, Figure 23 the reactive power at buses 6, Figure 24 shows the bus angle at all buses. Thus, there is a slight improvement in the voltage profile in the PV solar

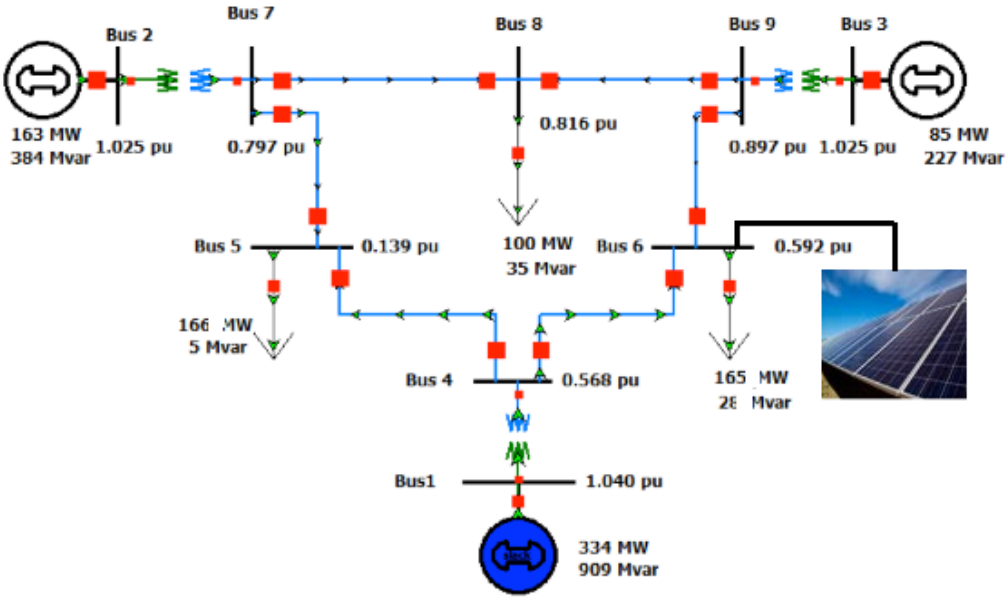

Figure 14: IEEE 9-Bus test systems with PV solar power plant penetration.

power plant integration as seen in Figure 19. Therefore, the system is in a state of stability, and all system variables do not exceed the permissible limits. It can be observed in Figure 15 that after the PV solar power plant is connected online to the system, the active and reactive power is no longer provided by the swing bus only. Both the swing bus and the PV solar power plant bus are contributed as shown in Figures 16 and Figure 18, respectively. It can be observed that PV solar power plants supply the most active and reactive power generation. Thus, the swing bus, bus 2, and bus 3 decreased their power capabilities, and the PV solar power plant helps the grid with power support and voltage regulation to the overall system.

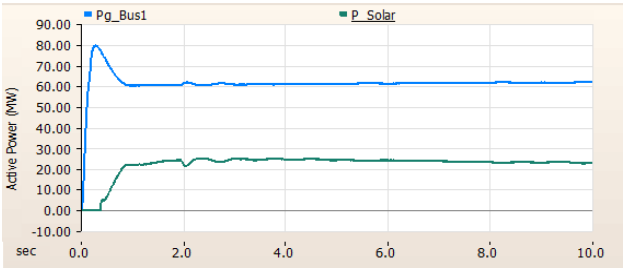

Figure 15: Active power generation at bus 1 (MW) with PV solar power plant connected.

4.2.2 System short-circuit

The third scenario investigates the transient responses of the sudden loss of the PV solar power plant connected to bus 6, and a symmetrical three-phase fault

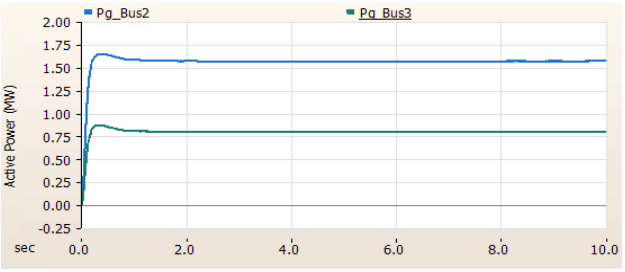

Figure 16: Active power generation at bus 2 & bus 3 (MW) with PV solar power plant connected.

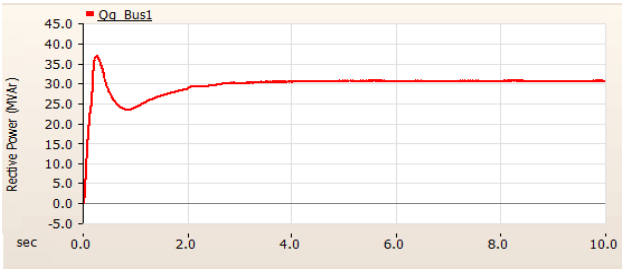

Figure 17: Reactive power generation at bus 1 (MW) with PV solar power plant connected.

was injected into the most loaded bus 8. The fault was initiated at 3 s and cleared at 3.2 s, as shown in Figure 25 and Figure 26. It created a severe drop in the active power synchronous generating system at the swing bus 1, bus 2, and bus 3, respectively. After 10 s, the generation stations reached 78 MW, 1.7 MW, and 0.9 MW, respectively. Figure 27 and Figure 28

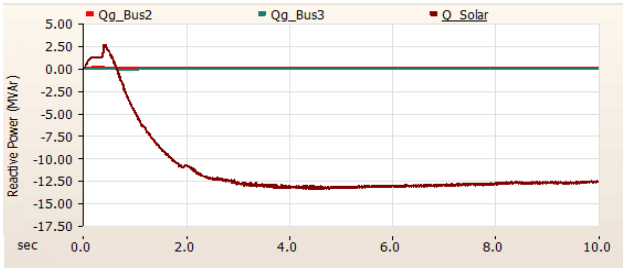

Figure 18: Reactive power generation at bus 2 & bus 3 (MVAR) with PV solar power plant connected.

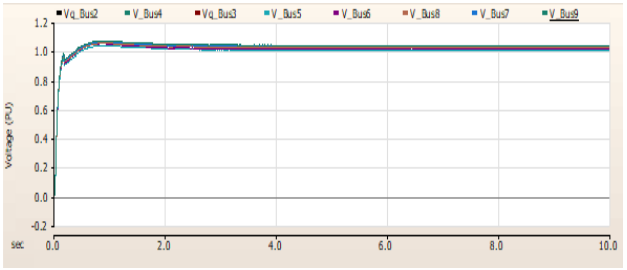

Figure 19: Voltage al all buses (pu) with PV solar power plant connected.

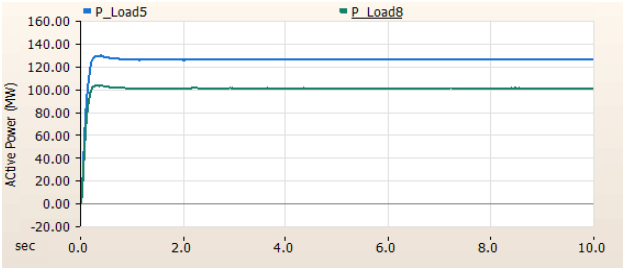

Figure 20: Active power at light load buses 5 & bus 8 (MW) with PV solar power plant connected.

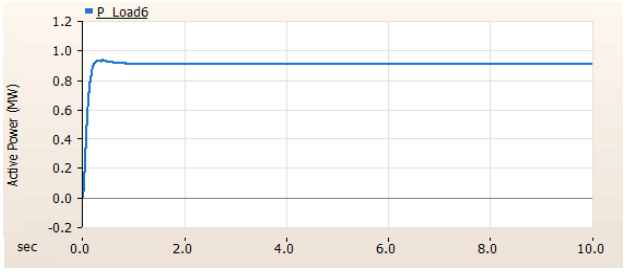

Figure 21: Active power at load bus 6- base case (MW) with PV solar power plant connected.

illustrate the variation in reactive power generation. The transient peaks of 100 MVAR, 1 MVAR, and 0.5 MVAR were detected at the swing bus and generator buses 2 and 3. Later, the transitory was wiped off in a short period. It was also observed that the active power generation decreased, with the reactive power

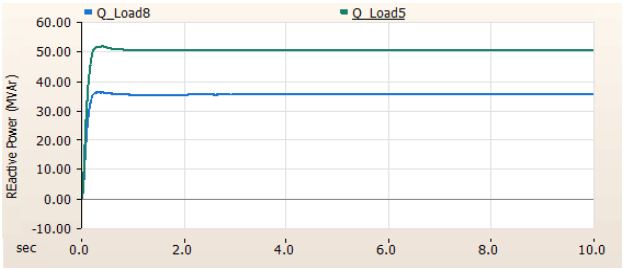

Figure 22: Reactive power at light load buses 5 & bus 8 (MVAR) with PV solar power plant connected.

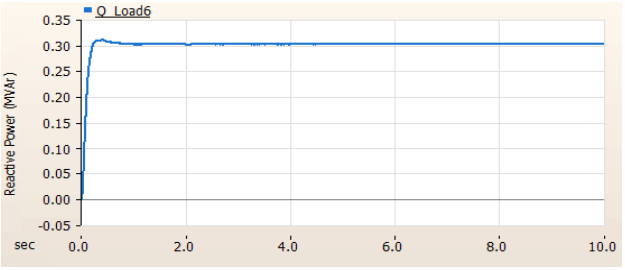

Figure 23: Reactive power at buses 6 (MVAR) with PV solar power plant connected.

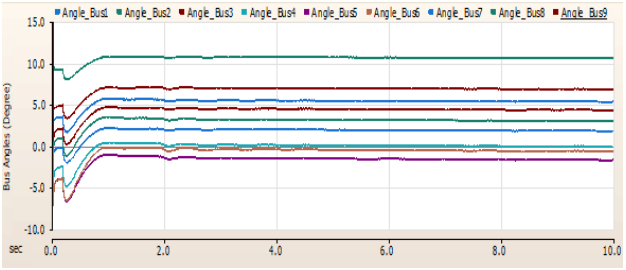

Figure 24: Buses angle with PV solar power plant connected.

generation at buses 1, 2, and 3 reaching a transitory peak of 4.12 pu. The voltage profile of the system's different buses is presented in Figure 29. A significant voltage drop was observed at bus 8 and bus 7, where the fault was injected. A declined voltage value of 0 p.u. was noted at the most loaded bus 8. Thus, an overall voltage drop to 0.4 in the grid is recorded. The changes in the real and reactive power values of load buses 5 & 8 were recorded and shown in Figures 30 and Figure 31, where the real power can be seen to have significantly dropped to 10 MW, 0.0 MW, and 0.1 MW, respectively. A severe oscillation in the reactive power demand at bus 8, as shown in Figure 32, reached 35 MVAR and damped within 1.2 sec. Reactive power at buses 6 (MVAR) with 3-ϕ SC at bas 8 and without PV solar power plant connected as shown in Figure 33.

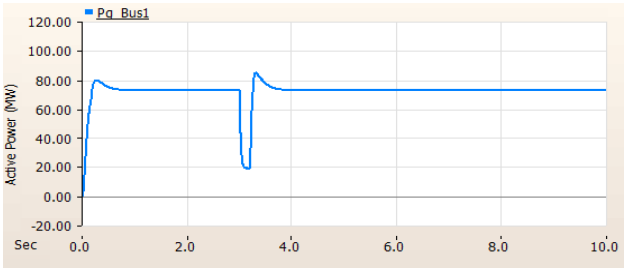

Figure 25: Active power at bus 1 (MW) with 3-ϕ SC at bas 8 and without PV solar power plant connected.

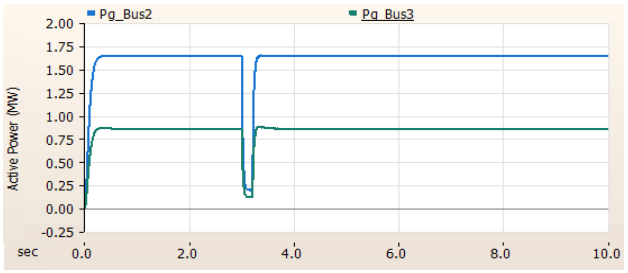

Figure 26: Active power at bus 2 & bus 3 (MW) with 3-ϕ SC at bas 8 and without PV solar power plant connected.

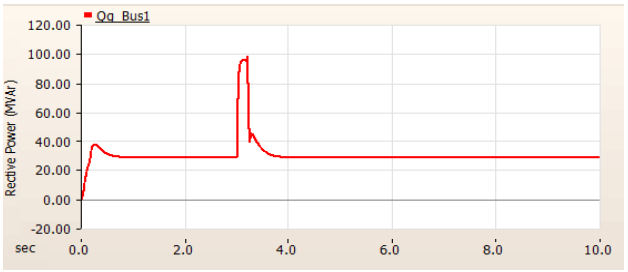

Figure 27: Reactive power at bus 1 (MVAR) with 3-ϕ SC at bas 8 and without PV solar power plant connected.

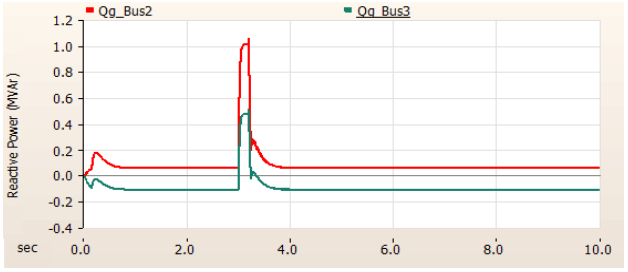

Figure 28: Reactive power at bus 2 & bus 3 with 3-ϕ SC at bas 8 and without PV solar power plant connected.

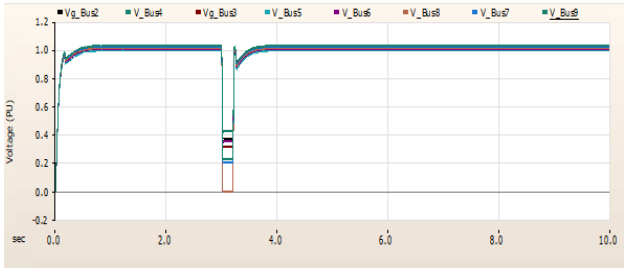

Figure 29: Voltage at all buses (pu) with 3-ϕ SC at bas 8 and without PV solar power plant connected.

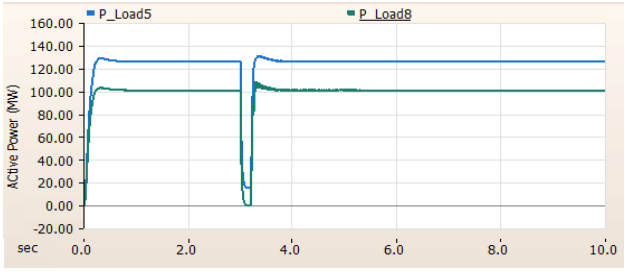

Figure 30: Active power at load bus 5 & bus 8 (MW) with 3-ϕ SC at bas 8 and without PV solar power plant connected.

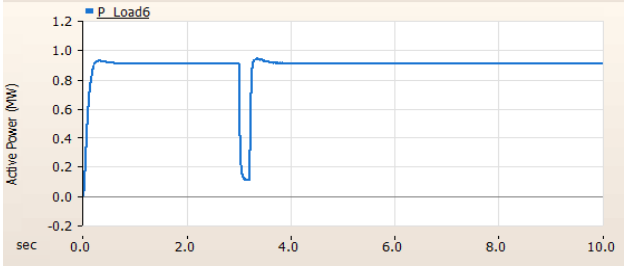

Figure 31: Active power at load bus 6- base case (MW) with 3-ϕ SC at bas 8 and without PV solar power plant connected.

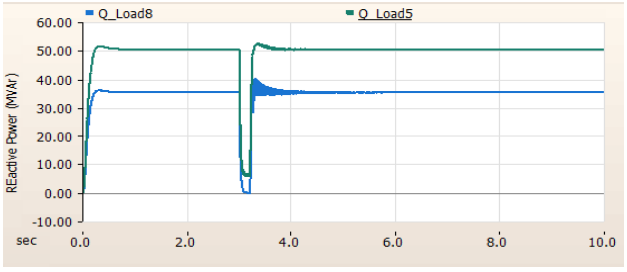

Figure 32: Reactive power at light load buses 5 & bus 8 (MVAR) with 3-ϕ SC at bas 8 and without PV solar power plant connected.

4.2.3 Voltage dip faults at PV solar power plant

In this scenario, a three-phase short circuit was applied at $t = 20$ s and cleared in 120 ms. Figure 34 shows the PV solar power plant bus voltage behavior for all the terminal bus locations during the fault-ride-through. Instantly after the occurrence of a fault,

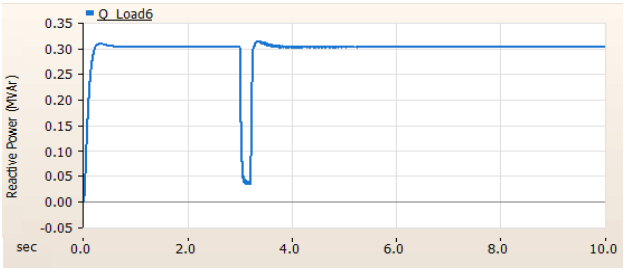

Figure 33: Reactive power at buses 6 (MVAR) with 3-ϕ SC at bas 8 and without PV solar power plant connected.

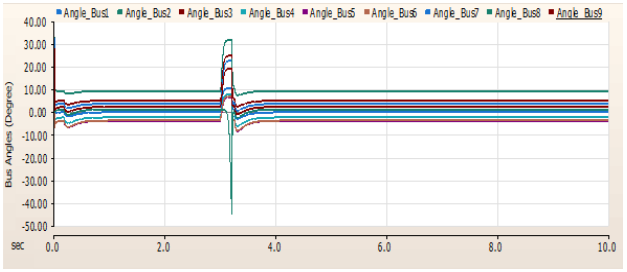

Figure 34: Voltage at all buses (pu) with 3-ϕ SC at bas 8 and without PV solar power plant connected.

the voltage at the PV bus drops from 1.0 p.u and at buses 5 and 8, respectively, to 0.2 p.u and 0.0 p.u according to the geographical distance of the respective PV farm. During the fault rides through, this voltage starts rising towards their rated values with an overshot in voltage at some buses: 5 and 8. These overshoots are because of the low capacity of those buses. Immediately after the fault is cleared at 5.120 s, as the PV farm begins a voltage regulation mode, the voltage at the PV terminal starts to reach its rated values. As demonstrated in Figures 35 and Figure 36, the active power generation at the PV solar power plant, swing bus 1, and generator buses 2 and 3 has experienced a dip reaching down to 0.2 pu due to a three-phase fault occurring at bus 8. Since a fast has protracted the PV bus, continuously acting controller by the schema of regulation. Thus, the voltage regulation at the PV bus is guaranteed. Figure 37 and Figure 38 depict a PV solar power plant bus's reactive power production pattern to provide voltage backing during the fault period. It is observed that the PV bus has contributed the most in supporting the system voltage regulation because the PV bus is the geographically nearest generating bus to the faulted bus 8. The results also show that the system is stable. Also, the power system has a good transient performance with rapid recovery of terminal voltage and reactive and active power during and after the fault clearance.

Figure 39 shows the bus voltage at all buses, Figure 40 shows the active power at load bus 5 & bus 8,

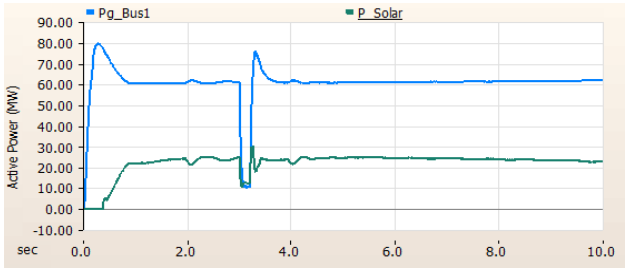

Figure 35: Active power at bus 1 (MW) with 3-ϕ SC at bas 8 and PV solar power plant connected.

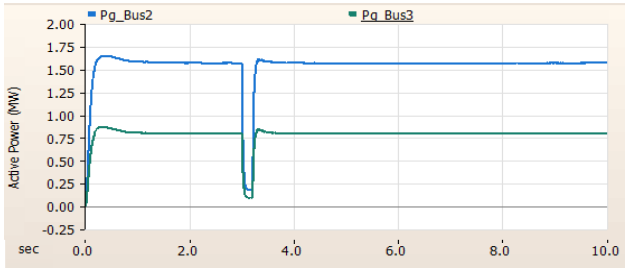

Figure 36: Active power at bus 2 & bus 3 (MW) with 3-ϕ SC at bas 8 and PV solar power plant connected.

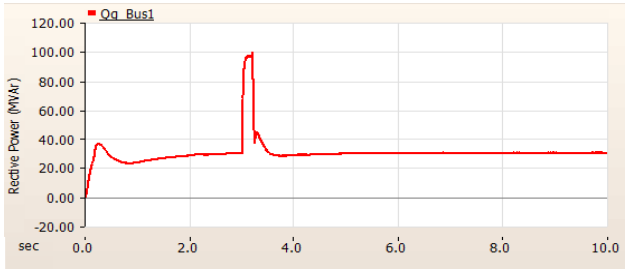

Figure 37: Reactive power at bus 1 (MVAR) with 3-ϕ SC at bas 8 and PV solar power plant connected.

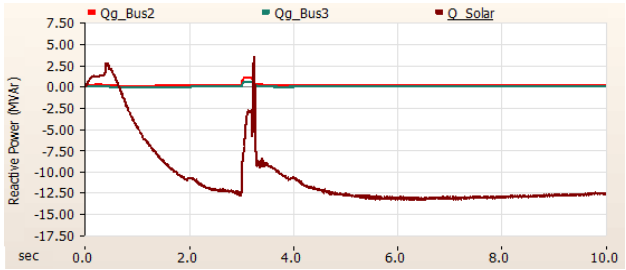

Figure 38: Reactive power at bus 2 & bus 3 with 3-ϕ SC at bas 8 and PV solar power plant connected.

Figure 41 shows the active power at load bus 6, Figure 42 shows the reactive power at light load buses 5 & bus 8, Figure 43 the reactive power at buses 6, Figure 44 shows the bus angle at all buses.

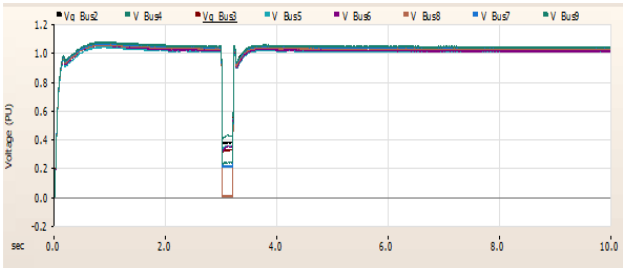

Figure 39: Voltage at all buses (pu) with 3-ϕ SC at bas 8 and PV solar power plant connected.

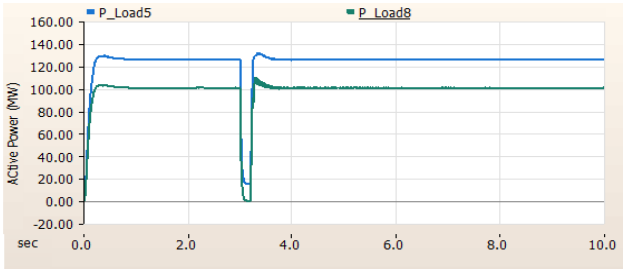

Figure 40: Active power at load bus 5 & bus 8 (MW) with 3-ϕ SC at bas 8 and PV solar power plant connected.

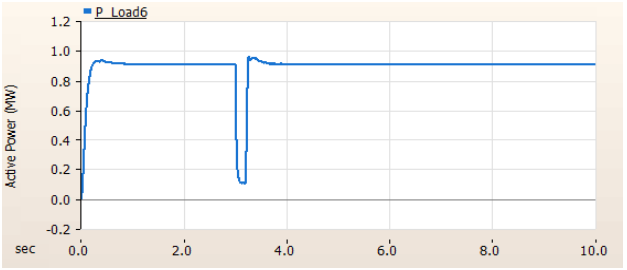

Figure 41: Active power at load bus 6- base case (MW) with 3-ϕ SC at bas 8 and PV solar power plant connected.

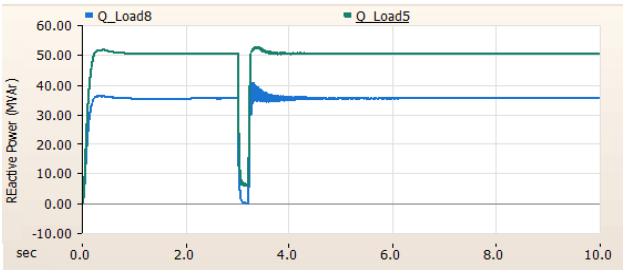

Figure 42: Reactive power at light load buses 5 & bus 8 (MVAR) with 3-ϕ SC at bas 8 and PV solar power plant connected.

5 Conclusion

This paper helped to create a test beds for transient stability study. The uniqueness of the proposed test

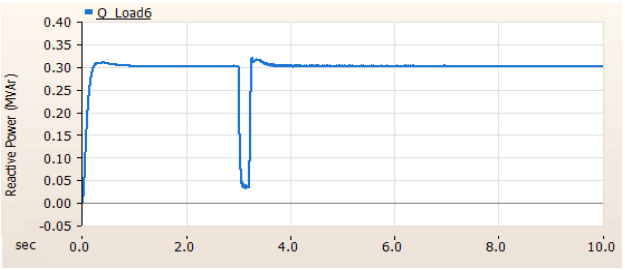

Figure 43: Reactive power at buses 6 (MVAR) with 3-ϕ SC at bas 8 and without PV solar power plant connected.

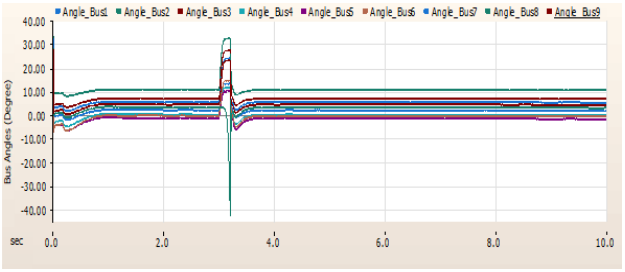

Figure 44: Voltage at all buses (pu) with 3-ϕ SC at bas 8 and PV solar power plant connected.

bed helped to validate the modeling of the IEEE 9-bus and the performance of a PV solar power plant for a variety of applications and validate the dynamic performance of the system. It demonstrated how the proposed test bed can be beneficial in investigating the impact of integrating the PV solar power plant. These scenarios helped in understanding the issues related to the increase of penetration of PV solar power plants to maximize electrical energy capacity, especially in weak systems, and increase the security and reliability of the grid as the PV solar system penetration grows. Thus, investigation of voltage stability demonstrates that the dynamic comportment of the voltage depends strangely on the short circuit capability of the transmission system at the bus of integration with the PV station. The dynamic performance of the grid has presented compliance with voltage ride-through capabilities that can be improved using a supplementary reactive supply. The extra generation of PV power has been found to considerably improve the voltage regulation, even in the case of over-voltages. Due to the additional reactive power absorption capacity offered by solar generators, a significant improvement in the system voltage regulation capability has been found. Due to the importance of the reactive power value obtained at the common coupling point with the grid, the reactive power contributions of SPV are taken into account. Abrupt disconnection of PV farms results in a voltage drop of 6% of the nominal voltage. Bus 8 has been mostly affected by this disruption, for which a

secondary frequency regulation action is necessary.

Further research may be carried out to address the following issues, such as developing detailed inverter-based solar models and controls to study and improve stability issues under fault conditions. Besides, additional variations of the load model could be considered. In particular, the mechanical torque of the induction motor load can be modified to, e.g., quadratic or a combination of different torque characteristics to form composite mechanical loads, which would affect short-term voltage stability. The additional operating points in the test system should be considered, e.g., PV systems that do not operate at unity power factor. Moreover, higher PV penetration levels are also of interest. Moreover, the studied contingencies could be varied in terms of fault location, fault impedance, fault type, or fault duration to affect different PV systems, induction motors, and synchronous generators in the test system. In continuation to the presented study, an extension has been intended to investigate the effects of different FACTS devices and the effect of environment temperature and irradiance on the dynamic voltage stability of the grid.

References:

[1] P. S. Kundur, *Power System Stability And Control*. McGraw-Hill, Inc, 2007.

[2] A. S. Saidi and M. I. Al-Rayif, "Impact of static and dynamic load model on the low voltage ride-through of the doubly-fed induction generator wind farm," *WSEAS Transactions on Power Systems*, vol. 12, pp. 1–10, 2017.

[3] K. Gunalan and C. Sharmeela, "A new control strategy to enhance LVRT for doubly fed induction generator," *WSEAS Transactions on Power Systems*, vol. 10, pp. 135–144, 2015.

[4] S. A. Adegoke and Y. Sun, "Power system optimization approach to mitigate voltage instability issues: A review," *Cogent Engineering*, vol. 10, 2023.

[5] A. G. Expósito and E. R. Ramos, "Augmented rectangular load flow model," *IEEE Transactions on Power Systems*, vol. 17, pp. 271–276, 2002.

[6] A. S. Saidi, F. Alsharari, E. M. Ahmed, S. F. Al-Gahtani, S. M. Irshad, and S. Alalwani, "Investigating the impact of grid-tied photovoltaic system in the Aljouf region, Saudi Arabia, using dynamic reactive power control," *Energies*, vol. 16, 2023.

[7] L. Zeng, H. D. Chiang, L. S. Neves, and L. F. C. Alberto, "On the accuracy of power flow and load margin calculation caused by incorrect logical PV/PQ switching: Analytics and improved methods," *International Journal of Electrical Power and Energy Systems*, vol. 147, 2023.

[8] J. Machowski, Z. Lubosny, J. Bialek, and J. Bumby, *Power System Dynamics: Stability and Control, 3rd Edition*. Wiley, 2020.

[9] J. Shair, H. Li, J. Hu, and X. Xie, "Power system stability issues, classifications and research prospects in the context of high-penetration of renewables and power electronics," *Renewable and Sustainable Energy Reviews*, vol. 145, 2021.

[10] Illinois Center for a Smarter Electric Grid, "Wscc 9-bus system." `https://icseg.iti.illinois.edu/wscc-9-bus-system/`, Last accessed on 22-12-2023.

[11] A. Gupta and R. K. Pachar, "A hybrid signal processing technique for identification and categorization of faults in IEEE-9 bus system," *Advanced Engineering Forum*, vol. 49, pp. 43–55, 2023.

[12] R. O. Olarewaju, A. S. Ogunjuyigbe, T. R. Ayodele, T. C. Mosetlhe, and A. A. Yusuff, "Assessing the voltage stability of power system in the presence of increasing solar PV penetration," in *IEEE AFRICON 2023, Nairobi, Kenya, September 20-22, 2023*, pp. 1–6, IEEE, 2023.

[13] Manitoba Hydro International Ltd., "Simple solar farm model written for PSCAD X4 version 4.6.3," 2019. `https://www.pscad.com/knowledge-base/download/simplesolarfarm2019.pdf`, Last accessed on 22-12-2023.

[14] N. U. Putri, F. Rossi, A. Jayadi, J. P. Sembiring, and H. Maulana, "Analysis of frequency stability with SCES's type of virtual inertia control for the IEEE 9 bus system," in *2021 International Conference on Computer Science, Information Technology, and Electrical Engineering, ICOMITEE 2021*, pp. 191–196, Institute of Electrical and Electronics Engineers Inc., 2021.

[15] N. Anwar, H. F. Khan, M. F. Ullah, and A. Hanif, "Transient stability analysis of the IEEE-9 bus system under multiple contingencies," *Engineering, Technology and Applied Science Research*, vol. 10, pp. 5925–5932, 2020.

[16] K. Loji, I. E. Davidson, and R. Tiako, "Voltage profile and power losses analysis on a modified IEEE 9-bus system with PV penetration

at the distribution ends," in *Proceedings - 2019 Southern African Universities Power Engineering Conference/Robotics and Mechatronics/Pattern Recognition Association of South Africa, SAUPEC/RobMech/PRASA 2019*, pp. 703–708, Institute of Electrical and Electronics Engineers Inc., 2019.

[17] O. Anaya-Lara and E. Acha, "Modeling and analysis of custom power systems by PSCAD/EMTDC," *IEEE Transactions on Power Delivery*, vol. 17, pp. 266–272, 2002.

[18] B. Gorgan, S. Busoi, G. Tanasescu, and P. V. Notingher, "PV plant modeling for power system integration using PSCAD software," in *2015 9th International Symposium on Advanced Topics in Electrical Engineering, ATEE 2015*, pp. 753–758, Institute of Electrical and Electronics Engineers Inc., 2015.

[19] L. Alhmoud, "Why does the PV solar power plant operate ineffectively?," *Energies*, vol. 16, 2023.

[20] S. Karmakar and B. Singh, "Multi-MPPT 72-pulse VSC based high-power grid interfaced solar PV plant with distributed DC-coupled battery energy storage," *IEEE Transactions on Energy Conversion*, 2023.

Contribution of Individual Authors to the Creation of a Scientific Article (Ghostwriting Policy)

Abdelaziz Salah Saidi: Formal analysis, Investigation, Methodology, Software, Supervision, Visualization, Writing – original draft. Osama Ali Zemi: Formal analysis, Investigation, Methodology, Software, Supervision, Validation. Lina Alhmoud: Methodology, Project administration, Supervision, Validation, Visualization, Writing – review & editing. Muhammad Umar Malik: Data curation, Formal analysis, Methodology, Resources, Software, Supervision.

Sources of Funding for Research Presented in a Scientific Article or Scientific Article Itself
Report potential sources of funding if there is any

No funding was received for conducting this study.

No Conflicts of Interest

The authors have no conflicts of interest to declare that are relevant to the content of this article.